Molecular-Beam Magnetic Resonance Studies of HD and D_2†

R. F. Code* and N. F. Ramsey
Lyman Laboratory of Physics, Harvard University, Cambridge, Massachusetts 02138
(Received 12 April 1971)

The results of some recent molecular-beam magnetic resonance experiments on HD and D_2 are reported. A discussion is given of the shifts and distortions of the separated oscillatory field resonance pattern produced by inhomogeneities in the external magnetic field and by the Bloch-Siegert effect. The sign of the electron-coupled spin-spin interaction constant in HD was remeasured to be positive. Its magnitude was determined to be 47(7) Hz. The spectrum of the $J=1$ state of D_2 was observed for external fields less than 160 G, and the spin-rotation and second-rank tensor interaction constants were determined to be $c_d = +8.768(3)$ and $d = +25.2414(14)$ kHz. Using the calculated value of $d'_M = +2.737(1)$ kHz for the magnetic spin-spin interaction constant, the value of the electric quadrupole interaction constant was determined from the observed value of d to be $eqQ/h = +225.044(24)$ kHz in the first rotational state of D_2. Hyperfine transitions were observed for the first time in the second rotational state of D_2. The hyperfine constants were determined from the transitions in the limit of zero external magnetic field to be $c_d = +8.723(20)$, $d'_M = 2.725(14)$, and $eqQ/h = +223.38(18)$ kHz in the second rotational state. The effects of isotopic substitution and nuclear motion on the hyperfine constants in molecular hydrogen are discussed.

I. INTRODUCTION

The magnetic properties and nuclear hyperfine interactions in the isotopic forms of the hydrogen molecule are determined with great accuracy by the molecular-beam magnetic resonance method. These experiments have a fundamental importance in the evaluation of quantum-mechanical descriptions of molecules and in the determination of the electric quadrupole moment of the deuteron Q_d. Since the original work on H_2 and D_2 by Kellogg, Rabi, Ramsey, and Zacharias,[1] significant advances have been made in experimental technique which improved the accuracy of the observations on the $J=1$ state of H_2 and D_2[2,3] and extended them to the $J=2$ state of H_2[3] and the $J=0$ and $J=1$ states of HD.[4,5] The present work has improved the accuracy of the observations on the $J=0$ state of HD and the $J=1$ state of D_2, and has observed the hyperfine interactions in the $J=2$ state of D_2 for the first time.

For the new experiments on the $J=0$ state of HD and the $J=1$ state of D_2, an effusive source was developed for producing molecular beams in the region of 20 °K. This source is temperature-regulated by the continuous transfer of helium vapor from an external liquid-helium Dewar, and is described in detail elsewhere.[6] Compared to the previous sources that were cooled by liquid nitrogen, this new low-temperature source has definite advantages. It reduces the instrumental linewidth by a factor of 2 and increases the deflecting power of the polarizing and analyzing magnets. The greater deflection power allows wider molecular beams to be used for the experiments and increases the signal to noise ratio of the resonances. This helium-cooled source is responsible for the increase in the precision of the molecular-beam determination of the sign of the electron-coupled spin-spin interaction constant δ in HD over the results obtained previously by Ozier *et al.*[4] using a liquid-nitrogen–cooled source on the same apparatus.

The low-temperature source was also used to observe the rf spectrum of the $J=1$ state of D_2 in low external magnetic fields. This was also the first time that D_2 had been observed at high precision with an electron bombardment detector, and nearly an order of magnitude increase in accuracy was achieved compared to the previous observations[2,3] in intermediate magnetic fields that used a Pirani gauge detector. This large increase in accuracy was obtained although no net decrease in instrumental linewidth compared to the previous observations was achieved in the new experiments. Although beam temperatures of 20 °K were used for the first time, the C magnet of the present apparatus is approximately one-half the length of the magnet used in the 1954 experiments that had a liquid-nitrogen–cooled source. Part of the increased accuracy is explained by improvements in the experimental signal to noise ratio, better stability of the external magnetic field, and by the observation of transitions in the low-field representation of the molecule. However, the most significant increase in accuracy came from the reduction of distortions in the separated oscillatory field resonance line shape, which allowed the line centers

to be determined with greater confidence.

The increased sensitivity of electron bombardment detection also made possible the observation of hyperfine transitions in the $J=2$ state of D_2 at a source temperature of 142 °K. These observations are interesting because of the effects of the nuclear spin symmetry of the deuterons. For even rotational levels of D_2 the nuclei must have a symmetric spin symmetry, and therefore the total nuclear spin I_R can be equal to zero or two. However, I_R is not a good quantum number for even rotational levels because states having $I_R=0$ are strongly mixed with states having $I_R=2$ by the hyperfine interactions. This is in contrast to the odd rotational levels where the nuclear spin symmetry is antisymmetric, and I_R has the unique value of 1. The nuclear magnetic spin-spin interaction constant d'_M and the electric quadrupole interaction constant eqQ/h cannot be determined independently from the hyperfine transitions in odd rotational levels because their matrix elements are proportional. But for even rotational levels, d'_M and eqQ/h can be determined independently by observing the hyperfine transitions specifically because I_R is not a good quantum number and strong mixing occurs. The present study of the hyperfine interactions in the $J=1$ and $J=2$ levels of D_2 is therefore a very interesting example of the effects of nuclear spin symmetry in molecules.

The comparison of the hyperfine interaction constants in the $J=1$ and $J=2$ rotational states of D_2 is also interesting because of the small differences that are caused by the effects of nuclear zero point motion and centrifugal stretching. These effects are significant in the present experiment, but cannot yet be calculated to the full precision of the observations on the $J=1$ state. Previous molecular-beam experiments on hydrogen molecules[2,3,5] compared the magnetic hyperfine properties of the $J=1$ states of H_2, HD, and D_2, as well as the $J=2$ state of H_2, by taking adiabatic averages over the nuclear motion. It is desirable to improve the method of calculating these effects, since the accuracy of the absolute value of Q_d is largely determined by uncertainties in the average values taken over the nuclear motion.[7] In addition, the nonequivalence of the two spin-rotation interaction constants observed in the $J=1$ state of HD suggests[5] that nonadiabatic effects of the nuclear motion may contribute amounts to the hyperfine constants that are measurable with present experimental accuracies. Unfortunately, only adiabatic methods[8-11] of calculating the effects of nuclear motion are presently available. It is therefore important to compare the values of Q_d determined from the new observations of the $J=1$ and $J=2$ states of D_2 with the value previously determined from the $J=1$ state of HD in assessing the reliability of the calculations.

II. LINE SHAPE

In the experiments on HD and D_2 using source temperatures of 18 °K, the signal to noise ratio was sufficiently great that the line centers could be located to within 1% of the linewidth. However, the resonance line shape must not be distorted or shifted from the value under ideal conditions in order for the experimental line centers to have meaning. Previous work[12] has shown that the distortions caused by inhomogeneities in the external magnetic field depend on the value of the rf perturbation. An additional distortion depending on the rf perturbation is caused by the Bloch-Siegert effect, which must be considered at low transition frequencies.

To estimate the effects of these distortions, it is necessary to determine the magnitude of the experimental rf magnetic field and the value of the velocity-averaged optimum rf perturbation. In this experiment it is also of interest to determine the velocity-averaged linewidth as a function of the beam temperature and rf perturbation to determine the performance of the low-temperature source. Therefore in this section some of the properties of the resonance line shape will be recalculated for the new experimental conditions, and an analysis will be given of a simple model for the shifts and distortions of the line shape.

The separated oscillatory field transition probability between two isolated states $|p\rangle$ and $|q\rangle$ has been previously discussed by Ramsey.[13] In general, the energy eigenvalues of the states W_p and W_q depend differently on the value of the external magnetic field, which may vary along the length of the resonance region in the C magnet. However, it is usually assumed that the external magnetic field is equal to the same constant value in each of the two rf regions, and although the external field may vary somewhat in the interference region that separates the two rf coils, its average value is assumed to be equal to the constant value in the rf regions. Note that this restriction on the average value of the field in the interference region will be removed when the model for distortions of the line shape is discussed.

When a rotating rf field of angular frequency ω, is applied coherently over the end regions with the above restrictions on the homogeneity of the external field in the rf regions, the transition probability for a single molecule with velocity v between two isolated states $|p\rangle$ and $|q\rangle$ is given by

$$P_{pq}(\omega;\ \omega_0,\ \bar{\omega}) = 4\sin^2\theta \sin^2\tfrac{1}{2}a\tau \times [\cos\tfrac{1}{2}\lambda T\cos\tfrac{1}{2}a\tau - \cos\theta \sin\tfrac{1}{2}a\tau \sin\tfrac{1}{2}\lambda T]^2, \quad (1)$$

where

$$\cos\theta = (\omega_0 - \omega)/a\ , \qquad \sin\theta = -2b/a\ ,$$
$$a = [(\omega_0 - \omega)^2 + (2b)^2\,]^{1/2}\ , \qquad \omega_0 = [(W_q - W_p)/\hbar]_{\substack{\text{rf}\\ \text{REGIONS}}}\ ,$$
$$\lambda = \bar{\omega} - \omega\ , \qquad \bar{\omega} = \int_0^L [(W_q - W_p)/\hbar L\,]\,dL'\ , \tag{2}$$
$$\tau = l/v\ , \qquad T = L/v\ .$$

Usually, ω_0 is a variable equal to $-\gamma H_{ext}$ at any point inside the magnet, but in these calculations it is more convenient to treat it as a constant equal to the angular frequency difference between the levels $|\,p\rangle$ and $|\,q\rangle$ in the two end rf regions. The frequency $\bar{\omega}$ is the average value of the frequency difference between the energy eigenvalues W_p and W_q in the interference region separating the two rf regions. The frequencies ω and b are related to the matrix element of the rf perturbation connecting the states $|\,p\rangle$ and $|\,q\rangle$ by the equation

$$\langle q\,|\,\mathcal{H}_{rf}\,|\,p\rangle = \hbar\, b\, e^{i\omega t}\ . \tag{3}$$

The distances l and L are the lengths of the individual rf field regions and the length of the interference region that separates them.

To simplify the averaging over the Maxwellian velocity distribution of the molecules in the effusive source, Eq. (1) is usually reduced to a sum of linear sine and cosine terms using standard trigonometric multiple angle formulas. The velocity-averaged transition probability can be expressed in terms of the basic integrals

$$I_n(x) = \int_0^\infty y^n\, e^{-y^2} \cos(x/y)\,dy,$$
$$K_n(x) = \int_0^\infty y^n\, e^{-y^2} \sin(x/y)\,dy. \tag{4}$$

The index n takes the values 2, 3, 4, or 5 depending on whether the beam detector is sensitive to the beam density, flux, momentum, or energy. The properties of these integrals are well known. The most recent discussion of them has been given by Harrison *et al.*[14] For the present experiment using electron bombardment detection, the correct index is $n = 2$.

For an undistorted line shape ($\omega_0 = \bar{\omega}$) and in the limit $L \gg l$, the optimum power and full width at half-maximum can be calculated for $n = 2$ using the method described by Ramsey[13] for the case $n = 3$. The results are that

$$2b_{opt} = 0.5165\pi\ \alpha/l\ \text{sec}^{-1} \quad \text{and} \quad \Delta\nu_{opt} = 0.557\,\alpha/L\ \text{Hz}. \tag{5}$$

These should be compared with the previous results for $n = 3$, namely, that

$$2b_{opt} = 0.600\pi\ \alpha/l\ \text{sec}^{-1} \quad \text{and} \quad \Delta\nu_{opt} = 0.65\ \alpha/L\ \text{Hz}. \tag{6}$$

It was also of interest to calculate the variation of linewidth as a function of the rf perturbation for the experimental conditions where the length of the rf regions is significant. For this calculation a numerical velocity average was taken of Eq. (1) and the ratio of L/l was set equal to the experimental value of 21.8. The results of this calculation are shown in Fig. 1. This calculation was helpful in determining the temperature of the beam from the resonance linewidth. It also explained why the resonance linewidth could not be profitably decreased by operating at low rf perturbations in the experiment. Although there is some decrease in linewidth at low values of the rf perturbations because molecules with slower velocities are favored, the decrease is not rapid enough to offset the loss of intensity at low rf perturbations. This is in part due to the poor velocity selection characteristics of a two-wire deflection field. Because of poor signal to noise ratios, the line centers could not be determined more accurately at low rf perturbations than at the optimum rf

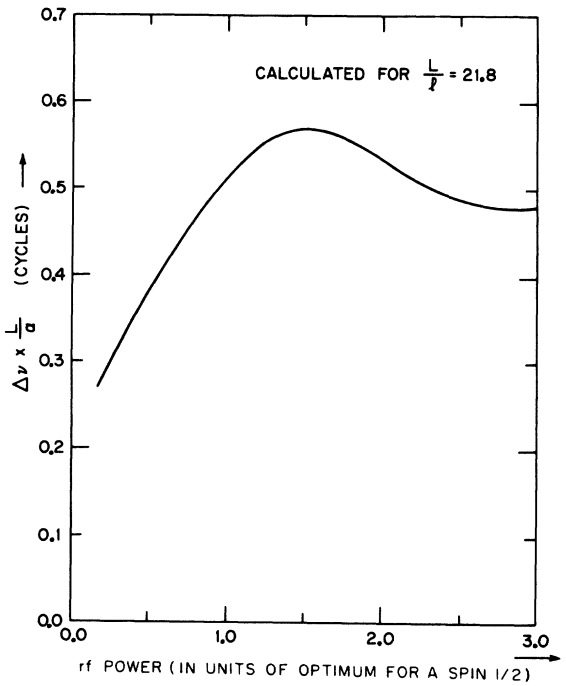

FIG. 1. Variation in linewidth of the separated oscillatory field resonance pattern for a spin $\frac{1}{2}$ as a function of the rf power.

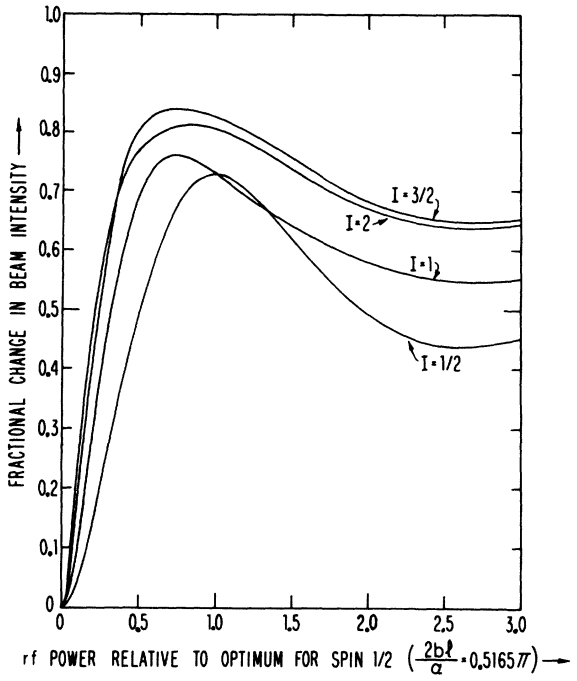

FIG. 2. Variation of intensity of resonances for spins $I=\frac{1}{2}$ to $I=2$ as a function of rf power using electron bombardment detection.

perturbation.

The rf magnetic field can easily be calibrated in terms of the current in the rf coil if the power response of a pure spin resonance is observed at exact resonance. For a spin $\frac{1}{2}$, the power response is given by

$$\langle P_{pq}\rangle = \tfrac{1}{2} - (2/\sqrt{\pi})\, I_2(4bl/\alpha). \tag{7}$$

This expression is plotted in Fig. 2. The power dependence of higher spin resonances is more complicated, but they can be calculated straightforwardly from Eq. (1) by using the Majorana formula[13] to generate the transition probabilities, and then taking the average over the velocity distribution of the beam. These results are also shown in Fig. 2 for spins up to $I=2$. Using these curves, the rf magnetic field can be calibrated from either the proton or deuteron resonances in the $J=0$ state of HD or from the deuteron resonance in the $J=0$ state of D_2. This calibration will be important later in determining the Bloch-Siegert shifts for the resonances. Also from the shape of the spin-$\frac{1}{2}$ response curve, the optimum power for a transition between two isolated levels $|p\rangle$ and $|q\rangle$ can be determined accurately.

We now turn to the model of line-shape distortions caused by inhomogeneity of the external magnetic field. We remark that Eq. (1) is still the exact transition probability for a single molecule when the average frequency difference between the levels $|p\rangle$ and $|q\rangle$ in the interference region $\bar{\omega}$ is not equal to the constant value ω_0 in the rf regions. However, in this case the line shape given by Eq. (1) is no longer symmetric, and its maximum value occurs at a frequency slightly different from $\bar{\omega}$. Since the line shapes can be conveniently calculated from Eq. (1) and its numerical velocity average when $\omega_0 \neq \bar{\omega}$, the model that we will use for shifts and distortions will assume that the external magnetic field is equal to the same constant value in each of the two rf regions, and that this value will be taken to be greater than the average value in the interference region. A qualitative description of the types of shifts that occur for the general case, when the external magnetic field is different in the two rf regions as well as in the interference region, should be given by this restricted model.

Therefore, if $\bar{\omega}$ is set equal to $\omega_0 - \delta$ in this model, where δ is a small shift in the average frequency difference of the states $|p\rangle$ and $|q\rangle$ in the interference region of the magnet such that $|\delta| \ll |2b|$, then the net shift of the resonance should vary linearly with δ for a specific rf power. The shifted resonance frequency will then be given by

$$\omega_r = \bar{\omega} + k\delta, \tag{8}$$

where k is an average factor whose magnitude should be approximately equal to l/L, since the molecules spend only a fraction of their total transit time in the rf regions where the external field is larger. However, the average factor k is influenced by the interference conditions between the two rf regions and it does not have a simple dependence on the rf perturbation.

For a single molecule near resonance under optimum rf conditions, the factor k can be evaluated from Eq. (1) by differentiation. This is similar to the approach used previously by Shirley.[15] In the limit that $L > l$, the center of the shifted resonance will coincide with the maximum value of Eq. (1). After taking the derivative and making suitable approximations, the shift factor k can be expressed as

$$k = l\tan x/(Lx + 2l\tan x). \tag{9}$$

Here, x is the measure of the rf perturbation, and is equal to $\frac{1}{2}a\tau$.

At the first optimum rf value, when $x=\frac{1}{4}\pi$, the value of k is approximately equal to $1.27\ l/L$, as expected. But at the next optimum, when $x=\frac{3}{4}\pi$, then k,is negative and approximately equal to $-0.42\ l/L$. It is apparent that $|k|$ decreases as x^{-1} when x is large and takes on an optimum value, and that k alternates in sign between successive optimum values of the rf perturbation.

Equation (9) is not valid when x is near a multiple of $\frac{1}{2}\pi$ for some fundamental reasons in addition to the approximations used in its derivation. At these

values of the rf perturbation, the interference pattern is a minimum on resonance. The inhomogeneity δ affects the shape of the nearby maxima more than it shifts the position of the minimum corresponding to resonance. The interference pattern is easily distorted, and the effects of a finite δ cannot be adequately described by a linear shift of the resonance as assumed in Eq. (7) for these rf perturbations.

The alternation of the sign of k for odd multiples of optimum power can be explained by the use of a rotating coordinate system.[13] Consider first the case of $x = \frac{1}{4}\pi$. In Fig. 3, the rotations of a spin $\frac{1}{2}$ with negative magnetic moment are shown in the frame rotating with the rf field at the resonance frequency ω_r. Because ω_r is less than ω_0, the effective magnetic field H_{eff} in the rf region is at an angle less than $\frac{1}{2}\pi$ from the point N on the sphere. The spin precesses $\frac{1}{2}\pi$ about H_{eff} from N to P in the first rf field. The next precession, occurring while the spin passes through the interference region, determines how close to the south pole the spin will be rotated by the second oscillatory field. The correct precession in the interference region for the resonance maximum is from P to Q clockwise about the north pole. This increases the relative angle between the spin and the oscillatory field in the second rf field sufficiently for the $\frac{1}{2}\pi$ rotation about H_{eff} to carry the spin down to the point R near the south pole. This clockwise precession means that the effective magnetic field in the interference region must point in the direction of the south pole, and hence ω_r must be greater than $\bar{\omega}$. If. however, the spin were to have precessed counterclockwise about the pole in the interference region, it would have rotated to Q', closer to the direction of H_{eff} in the rf regions, and the final position would be at the point R', which is further away from the point S than is the point R. Obviously, this would not be the correct direction for the spin to precess to obtain a resonance maximum in this case.

The precessions of the spin at resonance for the case $x = \frac{3}{4}\pi$ are not shown on Fig. 3, but they are related to those for $x = \frac{1}{4}\pi$ since a right-handed rotation about H_{eff} of $\frac{3}{2}\pi$ rad is equivalent to a left-handed rotation of $\frac{1}{2}\pi$ rad. Hence the path of the spin for $x = \frac{3}{4}\pi$ must resemble the mirror image of the path for the case $x = \frac{1}{4}\pi$ reflected in the plane containing H_{eff} and N. In particular, the precession in the interference region must be counterclockwise about the pole to move the spin the required amount away from the direction of H_{eff} in the second rf region. But this means that the direction of the effective field in the interference region must be toward the north pole, and therefore ω_r must be less than $\bar{\omega}$ and the sign of k must be negative in this case.

In an actual experiment, the average over the velocity distribution of the beam causes a smooth transition between positive and negative values of k near the vicinity of twice the optimum rf power, in contrast to the discontinuous behavior of Eq. (9). Therefore a numerical calculation of the shift factor k was done from Eq. (1) using the Maxwellian velocity distribution of the beam, and the results are shown in Fig. 4. The calculation parameters were $L/l = 21.8$ with a shift δ equal to $2.7\ \Delta\nu_{opt}$. The shift factor was calculated from Eq. (8) and was separately evaluated for the peak of the resonance and the midpoint of the first zero crossings of the 0–180° phase-shift pattern. The results show significant distortion of the line shape by the finite inhomogeneity δ near the vicinity of 1.5 times the optimum rf perturbation. The shift is apparently nonlinear in this region. However, the line shape becomes symmetrical again as the shift factor k goes through zero near 2.35 times the optimum rf perturbation.

The simplified model of line-shape distortion that we have been considering also describes the Bloch-Siegert effect on separated oscillatory field resonances. For a pure spin $\frac{1}{2}$ in a homogeneous external magnetic field H_0, the use of an oscillatory rf field of H_1 G rather than a rotating rf field shifts the resonance,[16] having the same effect an an increase in the external magnetic field in the rf regions of ΔH_{ext} G, where

$$\Delta H_{ext} = H_1^2/16 H_0 \ . \tag{10}$$

Therefore, the Bloch-Siegert effect is equivalent to a shift δ_{BS} between ω_0 and $\bar{\omega}$ which is proportional to the magnitude of the rf magnetic field. Shirley[15] has previously used an expression equivalent to Eq. (9) to calculate the Bloch-Siegert effect on separated

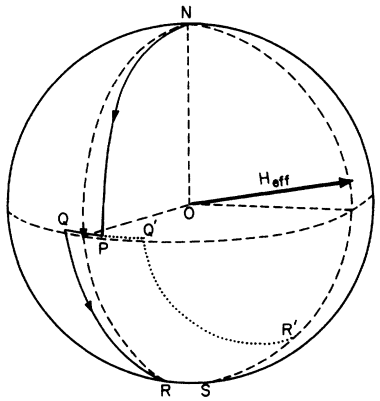

FIG. 3. Path in the rotating coordinate system of a spin $\frac{1}{2}$ for resonance at optimum rf power with a positive shift δ between the resonance frequency in the rf regions relative to the average field in the interference region. A negative magnetic moment is assumed. The explicit rotations are explained in the text.

oscillatory fields for a spin $\frac{1}{2}$ in a monochromatic beam at optimum rf perturbation. Note that for a transition between two isolated levels $|p\rangle$ and $|q\rangle$, the Bloch-Siegert shift can be calculated from Eq. (10) by making reference to the corresponding problem for a spin $\frac{1}{2}$ in an equivalent external magnetic field such that it has the same transition frequency and the same first-order dependence on the magnetic field.

For the present experiment, the velocity-averaged Bloch-Siegert shift may be calculated straightforwardly from Eq. (10) and the averaged values of k given in Fig. 4. In Fig. 5 we show the results of such a calculation, where the shift δ_{BS} has been taken equal to an arbitrary constant times the square of the rf perturbation. As before, in Fig. 4 the shifts of both the peak and middle of the resonance are shown. The velocity averaged Bloch-Siegert shifts appear to oscillate at high rf powers without increasing significantly in magnitude.

These calculations enable the shifts caused by magnetic field inhomogeneities and the Bloch-Siegert effect to be estimated for the separated oscillatory field resonances. However, corrections cannot be reliably made from this model because in actual experiments the external magnetic field varies inside the rf regions and does not necessarily have the same value in each of the two rf regions. Therefore, it is best to reduce the distortions as much as possible in an experiment by using end correction coils in the rf regions as in previous experiments.[2,3] For precise work, it is necessary to use small induction coils around the rf regions to trim the effective external magnetic fields in the rf regions such that the resonance frequencies in all three regions are equal to each other at the specific value of the rf current used to observe the particular resonance. Some useful tests for shifts of the resonances are to check the symmetry of the resonance peak and to determine whether the resonance frequency is sensitive to small variations in the rf perturbation.

III. EXPERIMENTAL METHOD

The basic molecular-beam apparatus used in these experiments has been described previously,[17] with the exception of a redesigned electron bombardment detector and its associated ultrahigh vacuum system.[18,19] The external magnetic fields of less than 160 G were stabilized over short terms to within ± 5 mG by a regulation system based on a Varian model FH-20 Hall effect gaussmeter. The helium-cooled source[6] was used for the observations on the $J=0$ state of HD and the $J=1$ state of D_2, while another effusive source[17] cooled to 142 °K by a freezing mixture of liquid pentane was used for the observations on the $J=2$ state of D_2. A HP 606A signal generator and a McIntosh 150-W audio amplifier were used for the rf system. The output of the amplifier was capacitively resonated with the rf coils to produce at least 4 A of current below 200 kHz. The eight turn rf coils were water cooled and were 1.8 cm in length. They were separated by a 39.3-cm-long interference region. End correction coils were used to trim the effective magnetic field equal in all three regions of the C magnet to reduce line shape distortions. The transition frequencies were measured by determining the frequency of points of equal height on either side of the resonance.

IV. SIGN OF δ IN HD

In response to some controversy a few years ago over the sign of the electron-coupled spin-spin interaction constant δ in HD,[20] a molecular-beam experiment was done by Ozier *et al.*[4] using a liquid-nitrogen–cooled source to measure the sign of this quantity. After the development of the present helium-cooled source, this experiment was repeated to take advantage of the increase of the spatial deflection of the beam and the decrease of the instrumental linewidth. The experimental method is similar to that used previously[21] to determine the sign of the spin-rotation constant in $^{13}C^{16}O$. The principle of this experiment, which measures the sign of δ relative to the sign of the proton magnetic moment, will now be described briefly.

In external magnetic fields greater than 1 G, the precession of the proton spin in the $J=0$ state of HD is uncoupled from that of the deuteron spin, and the Hamiltonian can be written in the high-field approximation as

$$\mathcal{H}/h = -g_p(\mu_N/h)m_p H_0 - g_d(\mu_N/h)\, m_d H_0 + \delta\, m_p m_d. \tag{11}$$

Here, μ_N is the nuclear magneton, and g_p, m_p, g_d, and m_d are the nuclear g factors and z components of the spins of the proton and deutron, respectively.

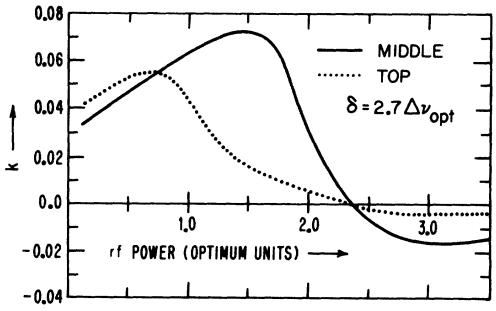

FIG. 4. Dependence of the average factor k on the rf power calculated for $L/l = 21.8$ and $\delta = 2.7\Delta\nu_{opt}$. The solid line represents the shift of the midpoint of the resonance and the dotted line represents the shift of the peak of the resonance.

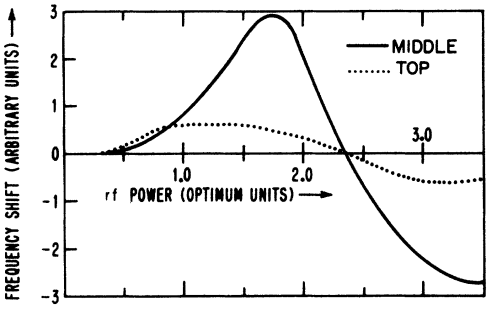

FIG. 5. Typical variation of the Bloch-Siegert shift for separated oscillatory fields as a function of rf power. The calculation is based on the results of Fig. 4.

The magnitude of the deuteron resonance frequency in the external magnetic field depends on the values of m_p and δ by the equation

$$|\nu_d| = g_d(\mu_N/h)H_0 - \delta m_p . \quad (12)$$

The basis of the present molecular-beam measurement is that the two proton spin states in the $J=0$ level of HD are separated by the deflecting magnetic field gradients in the A and B magnets. This occurs because the proton magnetic moment $\frac{1}{2}g_p\mu_N$ is greater than the deuteron magnetic moment $g_d\mu_N$ and, therefore, the effective magnetic moment in the $J=0$ state along the external field, given by

$$(\mu_{eff})_z = (g_p m_p + g_d m_d)\mu_N , \quad (13)$$

has the same sign as m_p since g_p is positive.

The direction of the deflecting force on the molecule is therefore determined by the sign of m_p and the sign of the magnetic field gradient $(\partial H_0/\partial z)$, since

$$F_z = (\mu_{eff})_z \left(\frac{\partial H_0}{\partial z}\right) . \quad (14)$$

A diagram of the state selection of the positive proton component of the $J=0$ state of HD by placing obstacles in the beam is shown in Fig. 6. The relative directions of H_0 and $\partial H_0/\partial z$ in the magnets are also shown in the diagram. It can be seen that the portion of the beam whose sigmoid path lies on the groove side of the deflecting magnets consists of molecules that have only positive values of m_p. The m_p states are selected by moving a particular buffer slit at the exit of the B magnet more than halfway into the beam to allow only the desired m_p state to pass through to the detector.

The deuteron resonance was observed in an external magnetic field of 156.68 G. The separated oscillatory field resonance occurred at 102.40 kHz, and the single-coil transition frequencies in the two rf regions were trimmed by the correction coils to be 102.5 and 102.7 kHz, respectively, for the same value of the rf current that was used to observe the separated oscillatory field resonance. The separated oscillatory field resonance linewidth using the helium-cooled source was approximately 475 Hz. In each case the deuteron resonance frequency was higher for the $m_p = -\frac{1}{2}$ states (selected by moving the buffer slit on the groove side of the B magnet into the beam to obstruct at least 75% of the total beam intensity) than for the $m_p = +\frac{1}{2}$ states, reconfirming that δ is positive.

The statistical result of the experiment was that $\delta = +47(3)$ Hz, where 3 Hz is 1 standard deviation. A small systematic error can arise from the asymmetries in the line shape since it is difficult to measure the center frequencies of the two shifted resonances at the same relative position. The magnitude of this error can be estimated from the calculations of the factor k in Sec. II to be approximately 4 Hz. The final result of the present molecular-beam experiment is therefore

$$\delta = +47(7) \text{ Hz}.$$

(Here and elsewhere in this paper, quantities in parentheses following a number indicate the uncertainty of the last printed numeral of the preceding number. The uncertainties are expressed as probable errors.)

An independent nuclear magnetic resonance (NMR) measurement by Benoit *et al.*[22] has also been able to measure the sign of δ relative to the sign of the proton magnetic moment. This experiment observed the NMR of liquid HD at frequencies of 54 and 74 Hz in variable external magnetic fields less than 30 mG. In addition to confirming the

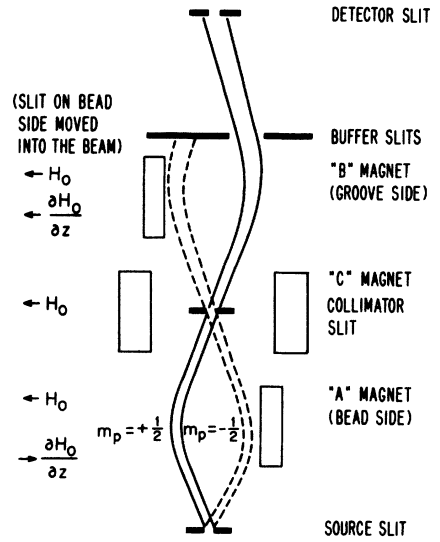

FIG. 6. Technique for state selection of the $m_p = +\frac{1}{2}$ states in the $J=0$ level of HD for determining the sign of the electron-coupled spin-spin interaction constant.

positive sign of δ, this NMR experiment has determined the most accurate value for δ presently available by observations in an external field of 1.5 G, with the result that $\delta = +42.94(10)$ Hz.

Some progress has been made in the theoretical calculations of δ in recent years, and a new value of +42.57 Hz has been reported.[23] The agreement between theory and experiment is now very good. While the present molecular-beam experiment does not provide the best measurement of the magnitude of δ in HD, it has definitely established the sign by a very fundamental technique, which can be applied to measure the sign of δ in similar molecules such as HCl.

V. $J = 1$ STATE OF D_2

In the present work, the rf spectrum of the $J = 1$ state of D_2 was studied in low magnetic fields using the helium-cooled source. These fields were low enough that the magnetic susceptibility of the molecule could be neglected. In addition, the transition frequencies could be calculated to sufficient accuracy by using the value of the rotational magnetic moment determined by the previous high-field experiment,[3] and by considering only the average value of the shielding constant of the nucleus.

With these low-field approximations, the Hamiltonian of the $J = 1$ state of D_2 can be written as

$$\mathcal{H}/h = -(1-\sigma)g_d(\mu_N/h)\vec{I}_R\cdot\vec{H} - g_J(\mu_N/h)\vec{J}\cdot\vec{H} - c_d\vec{I}_R\cdot\vec{J} + [5d/(2J-1)(2J+3)] \times [3(\vec{I}_R\cdot\vec{J})^2 + \tfrac{3}{2}(\vec{I}_R\cdot\vec{J}) - \vec{I}_R^2\vec{J}^2] \ . \quad (15)$$

Here, I_R is the total resultant nuclear spin, which is a good quantum number in the case of D_2 for odd rotational levels only where I_R is equal to unity. The quantity σ is the average value of the nuclear shielding constant, $\vec{H}$ is the external magnetic field, g_J is the rotational g factor of the molecule, and c_d is the deuteron spin-rotation interaction constant. The constant d is defined as

$$d = \frac{egQ}{10h} + \frac{2}{5}\frac{(g_d\mu_N)^2}{h}\ {}^{D_2}_{0}\left\langle \frac{1}{R^3}\right\rangle_1 , \quad (16)$$

where eqQ is the electric quadrupole coupling constant in the molecule and R is the internuclear distance. Only this linear combination of the electric quadrupole and spin-spin interaction constants can be determined from the hyperfine transitions in the $J = 1$ state of D_2.

The matrix elements of the Hamiltonian given in Eq. (15) have previously been discussed by Ramsey[24] along with the calculation of the energy levels in intermediate fields. A diagram of the hyperfine energy levels of the $J = 1$ state of D_2 in external magnetic fields up to 160 G is shown in Fig. 7. The energy levels have been identified with the notation used by Ramsey. The energy levels are approximately linear in this region, and a good extrapolation to the zero-field transition frequencies can be made.

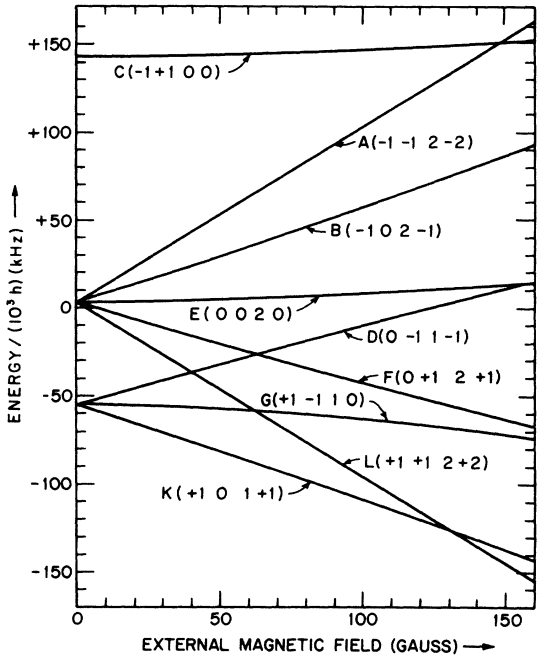

FIG. 7. Plot of the energy levels (in kHz) of the $J = 1$ state of D_2 in low magnetic fields. The states are labeled $A(m_I m_J F m_F)$.

Some of the allowed transitions in the low-field limit ($\Delta F = \pm 1, 0$; $\Delta m_F = \pm 1$) could not be used to determine c_d or d. An overlap of the interference patterns occurred for the line pairs AB/GK and FL/DG. The transitions BE and EF were resolved from each other, but were significantly shifted because all three levels B, E, and F are connected by the rf perturbation. The transition CD could not be observed because there was an accidental cancellation of the change in the molecular effective magnetic moment in the deflecting magnets. For external fields above 75 G, the transition CF, which is allowed in the high-field limit, can be observed in place of CD.

The five transitions CK, CF, BG, EK, and AD were observed for the determinations of c_d and d. A recorder trace of the transition AD is shown in Fig. 8. The signal to noise ratio on this resonance is representative of that observed for the other transitions in the $J = 1$ state of D_2 using the helium-cooled source.

In a preliminary version of the experiment that did not use end correction coils, the external magnetic fields in the two rf regions were not equal to

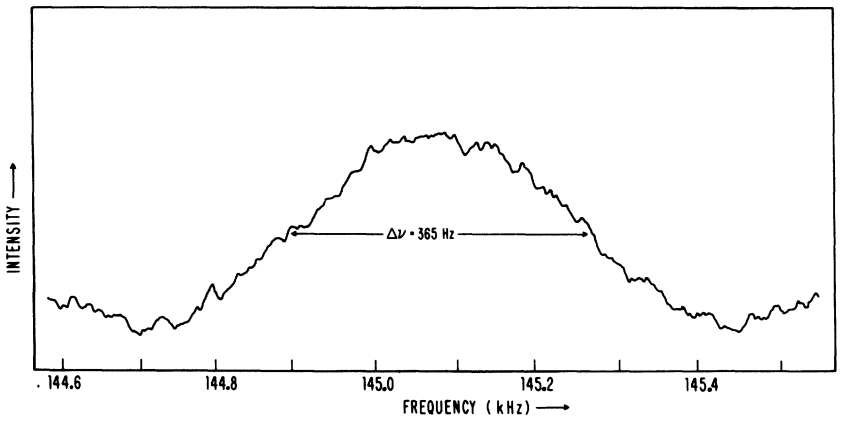

FIG. 8. The transition AD in the $J=1$ state of D_2 observed with an 8-sec time constant. The external field was approximately 157 G and the error in determining the line center is ±5 Hz.

each other, nor equal to the average value of the field in the interference region. Part of these inhomogeneities were caused by the iron yoke of the C magnet, and part were caused by the fringing fields of the nearby A and B deflecting magnets. The resonances were shifted significantly by these inhomogeneities, and data taken at different values of the external magnetic field yielded inconsistent values of c_d and d.

In the final version of the experiment these systematic errors were reduced to a tolerable level by trimming the external fields in the rf regions with end correction coils as recommended at the end of Sec. II. The Bloch-Siegert effect, which is the other source of systematic error in these observations, was estimated to be less than 4 Hz for all transitions. Since this is approximately 1% of the separated oscillatory field linewidth, no corrections were made for these shifts in the analysis.

The summary of the experimental data is shown in Table I. The value of the external magnetic field was calibrated by observing the deuteron resonance in the $J=0$ state of D_2. The data were analyzed by setting $(1-\sigma)\,g_d$ equal to 0.857392[25] and g_J equal to 0.442884[3] and then performing a least-squares fit with respect to c_d and d. The standard deviation of the fit to the data was 3.3 Hz, indicating a high degree of consistency in the observations. The best estimates for c_d and d are

$$c_d = +8.768(3)\ \text{kHz}$$

and

$$d = +25.2414(14)\ \text{kHz},$$

where the errors indicated are an estimate of 1 standard deviation of the total statistical and systematic errors.

Using these values of the hyperfine constants, the two zero-field transition frequencies for the $J=1$ level of D_2 were determined to be 198.078 kHz for the $F=0$ to $F=1$ line and 58.187 kHz for the $F=1$ to $F=2$ line with an uncertainty of 10 Hz. The limit of zero external magnetic field was desired for the observations on the $J=2$ level of D_2, but it was not possible to achieve this limit by a simple demagnetization because of the residual fields from the iron yoke of the magnet that could not be removed in the experiment. Therefore, the limit of zero field was established by observing the hyperfine transitions of the $J=1$ level of D_2, and adjusting the current in the magnet winding and in the two end correction coils until the zero-field frequencies were obtained in all three regions of the magnet. The line CK was of particular value for this field calibration because it is the only observable transition between the $F=0$ and $F=1$ states. The sudden transitions that occur when the molecules pass through regions of zero field make this transition frequency a linear function of the magnet current. After the limit of zero field had been established by observing the line CK, the frequency of the other hyperfine transition between the $F=1$ and $F=2$ states was measured and found to be in excellent agreement with the calculated zero-field value.

VI. $J=2$ STATE OF D_2

The earlier molecular-beam measurement[3] of

TABLE I. Observations of transition frequencies (in kHz) in the $J=1$ state of D_2 in the low magnetic fields.

Transition	$H_0=156.672$[a] (G)	$H_0=92.490$[b] (G)	$H_0=92.433$[c] (G)
CK	292.965(4)	250.239(3)	250.204(2)
CF	216.572(8)	185.126(5)	185.095(2)
BG	163.171(8)	114.618(4)	114.576(2)
EK	155.036(7)	111.756(2)	111.720(2)
AD	144.935(4)	107.492(3)	107.464(3)

[a]Entries in this column are average values of four sets of observations.

[b]Entries in this column are average values of six sets of observations.

[c]Entries in this column are average values of five sets of observations.

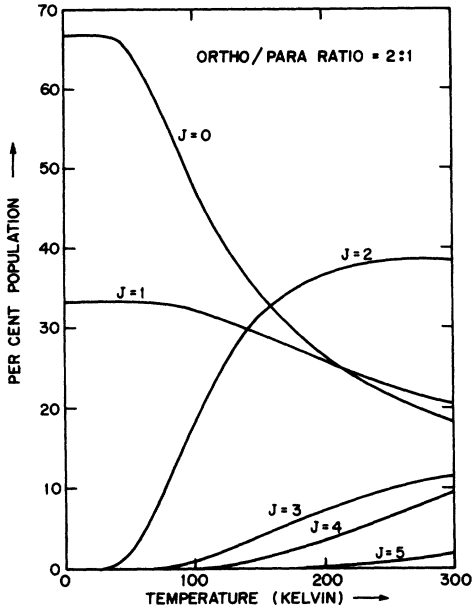

FIG. 9. Total population in the rotational states of D_2 as a function of temperature.

the rotational magnetic moment in the second rotational state of H_2 suggested that the hyperfine interactions in the second rotational state of D_2 could be observed with an electron-bombardment detector. The distribution of rotational states in D_2 as a function of temperature is shown in Fig. 9 assuming an ortho/para ratio of 2/1. Above 200 °K, the deflections for D_2 in the present apparatus are too small for the transitions to be easily detected, so that the most efficient range of source temperatures to observe the hyperfine transitions in the $J=2$ state of D_2 is between 140 and 190 °K.

However, there are 30 hyperfine levels in the second rotational state of D_2, so that in a large external magnetic field the spectrum would be complicated and each transition would have only a very small intensity. Therefore, the hyperfine spectrum was observed in the limit of zero external magnetic field, where there are only six different energy levels, and the degeneracies increase the strength of the observed resonances.

If the nuclei of D_2 are treated for the moment as distinguishable particles, the nuclear spin Hamiltonian in the limit of zero external magnetic field can be written as

$$\mathcal{H}/h = -c_d(\vec{I}_1+\vec{I}_2)\cdot\vec{J} - \tfrac{5}{2}\sqrt{6}\,\overleftrightarrow{C}^{(2)}\cdot\{I_1, I_2\}^{(2)} + \overleftrightarrow{V}_1\cdot\overleftrightarrow{Q}(I_1)/h + \overleftrightarrow{V}_2\cdot\overleftrightarrow{Q}(I_2)/h\ , \quad (17)$$

where the tensor notation of Edmonds[26] has been used. The quantity c_d is the spin-rotation constant of the deuterons and d'_M is the magnetic spin-spin interaction constant defined by

$$d'_M = \frac{2}{5}\left(\frac{\mu_1}{I_1}\right)\left(\frac{\mu_2}{I_2}\right)\frac{1}{h}\,{}_v\!\left\langle\frac{1}{R^3}\right\rangle_J\ . \quad (18)$$

The last two terms in Eq. (17) are the interaction energies between the electric quadrupole moments of the two nuclei and the gradient of the electric field at the nuclear sites.

Because of the identity of the nuclei in D_2, it is convenient to calculate the matrix elements of $\mathcal{H}$ with respect to basis wave functions with definite total resultant nuclear spin $\vec{I}_R=\vec{I}_1+\vec{I}_2$, since these wave functions are either symmetric or antisymmetric with respect to an interchange of the two nuclei. The deuterons obey Bose statistics, so that only the symmetric nuclear wave functions (with I_R equal to 0 or 2) are allowed for the second rotational state. The complete basis states used for the matrix of $\mathcal{H}$ in zero field will be the set $|(I_1, I_2)I_R, J, F\rangle$, where

$$\vec{F}=\vec{I}_R+\vec{J}\ . \quad (19)$$

Unlike the case for odd J values, the Hamiltonian is not diagonal in this basis because of the mixing of $I_R=2$ states with $I_R=0$ states caused by the hyperfine interactions. It is this mixing that allows the electric quadrupole interaction to be determined separately from the magnetic spin-spin interaction in the $J=2$ state of D_2. The interesting effects of nuclear spin symmetry in D_2 are that for even values of J these two second-rank-tensor hyperfine interactions are distinguishable from each other, while for odd values of J they become indistinguishable.

The nonzero matrix elements of the Hamiltonian given in Eq. (17) can be calculated from the following formulas[26]:

$$\langle I_R, J, F|\,-c_d\vec{I}_R\cdot\vec{J}\,|I_R, J, F\rangle = -c_d\left(\frac{I_R(I_R+1)+J(J+1)-F(F+1)}{2}\right)\ , \quad (20)$$

$$\langle I'_R, J, F|\,-\tfrac{5}{2}\sqrt{6}\,d'_M\,\overleftrightarrow{C}^{(2)}\cdot\{I_1, I_2\}^{(2)}\,|I_R, J, F\rangle = -15\sqrt{30}\,d'_M(-)^{F+I_R+J}(2J+1) \times\begin{pmatrix}J&2&J\\0&0&0\end{pmatrix}[(2I_R+1)(2I'_R+1)]^{1/2}\begin{Bmatrix}F&J&I'_R\\2&I_R&J\end{Bmatrix}\begin{Bmatrix}1&1&1\\1&1&1\\I'_R&I_R&2\end{Bmatrix}\ , \quad (21)$$

and

$$(1/h)\langle I'_R, J, F \,|\, \vec{V}_1 \cdot \vec{Q}(I_1) + \vec{V}_2 \cdot \vec{Q}(I_2) \,|\, I_R, J, F\rangle = (2/h)\langle |\, \vec{V}_1 \cdot \vec{Q}(I_1) \,|\rangle = \frac{2eqQ}{4h} (-)^{2I_R+J+F+1}$$

$$\times \left(\frac{(2I_R+1)(2I'_R+1)J(J+1)(2J+1)15}{(2J-1)(2J+3)}\right)^{1/2} \begin{Bmatrix} 1 & I'_R & 1 \\ I_R & 1 & 2 \end{Bmatrix} \begin{Bmatrix} F & J & I'_R \\ 2 & I_R & J \end{Bmatrix} . \quad (22)$$

The values of $3-j$ and $6-j$ symbols are given in the tables by Rotenberg *et al.*[27] The $9-j$ symbol can be calculated easily from an appropriate sum over triple products of $6-j$ symbols.

The matrix elements of Eq. (17) are listed in Table II. Note that there are two basis states that have the total angular momentum $\vec{F}$ equal to two, and that these states are mixed strongly together by the off-diagonal matrix elements of the spin-spin and electric quadrupole interactions. The eigenstates of this two-dimensional manifold will be denoted by $|F = 2_+\rangle$. Therefore, there are six eigenstates and six allowed transitions in zero field. It is sufficient to observe at least three of these transitions in order to determine the values of c_d, d'_M, and eqQ/h in the second rotational state.

Four of the six possible transitions were observed in the present experiment. Recorder tracings of these resonances are shown in Fig. 10. Because the temperature of the source was 142 °K for these observations, the resonances had to be induced with much larger rf perturbations than were used for the observations of the $J=1$ state of D_2 at 20 °K. The average rf current used was 8 A, the maximum output of the audio amplifer in this frequency range. The average magnetic field was set to within 25 mG of the desired zero value by observing the hyperfine transitions of the $J=1$ state of D_2 as described at the end of Sec. V.

The major difficulty in determining the center frequency of the transitions is caused by the overlap of parts of the interference patterns of some of the resonances. Since the full width of the resonances at half-maximum was 1.1 kHz, part of the secondary maximum of the $J=1$ hyperfine transition at 58.187 kHz overlapped with the $F=2_+$ to $F=3$ transition in the second rotational state. Overlap also occurred between the $F=1$ to $F=2_+$ transition and the $F=3$ to $F=4$ transition. The shifts caused by the overlap of the interference patterns can be estimated graphically, and are greater than the shifts caused by the inhomogeneity of the external magnetic field and by the Bloch-Siegert effect. The inhomogeneity shifts were estimated to be less than the statistical errors in determining the line centers. The largest Bloch-Siegert shift occurs for the $F=0$ to $F=1$ transition and is less than 35 Hz for an rf current of 10 A. The overlap shifts are approximately 50 Hz in magnitude.

TABLE II. Matrix elements of the nuclear spin Hamiltonian in the second rotational state of D_2 in zero external field.

Matrix elements $\langle I'_R\ J\ F \,|\, (\mathcal{H}/h) \,|\, I_R\ J\ F\rangle$	
$\langle 2\ 2\ 4 \,|\, (\mathcal{H}/h) \,|\, 2\ 2\ 4\rangle =$	$-4\ c_d + 10\ d'_M/7 - eqQ/7h$
$\langle 2\ 2\ 3 \,|\, (\mathcal{H}/h) \,|\, 2\ 2\ 3\rangle =$	$-20\ d'_M/7 + 2\ eqQ/7h$
$\langle 2\ 2\ 2 \,|\, (\mathcal{H}/h) \,|\, 2\ 2\ 2\rangle =$	$3\ c_d - 15\ d'_M/14 + 3\ eqQ/28h$
$\langle 0\ 2\ 2 \,|\, (\mathcal{H}/h) \,|\, 0\ 2\ 2\rangle =$	0
$\langle 2\ 2\ 1 \,|\, (\mathcal{H}/h) \,|\, 2\ 2\ 1\rangle =$	$5\ c_d + 5\ d'_M/2 - eqQ/4h$
$\langle 2\ 2\ 0 \,|\, (\mathcal{H}/h) \,|\, 2\ 2\ 0\rangle =$	$6\ c_d + 5\ d'_M - eqQ/2h$
$\langle 0\ 2\ 2 \,|\, (\mathcal{H}/h) \,|\, 2\ 2\ 2\rangle =$	$(1/\sqrt{7})\ (5\ d'_M + eqQ/h)$

The experimental data for the zero-field transition frequencies in the second rotational state of D_2 are shown in Table III. For each transition two frequencies are shown: The first is the uncorrected measurement, and the second is a corrected value for the effects of the overlap of the resonance line shapes. Since the $F=0$ to $F=1$ transition was quite weak and was subject to the largest Bloch-Siegert shift, the frequencies of three stronger lines were remeasured at slightly lower than optimum rf perturbation to check the consistency of the first observations. The hyperfine constants determined from these two sets of data, with and without the overlap shift corrections applied, were all self-consistent.

The corrections for the overlap errors were difficult to make because the width of the interference pattern depends on the rf power used to observe the transitions. Since it was uncertain whether the overlap corrections improved the accuracy of the determination of the hyperfine constants, the final values for the hyperfine constants were taken as the averages of the determinations from the corrected and uncorrected data, with the result that

$$c_d = 8.723(20) \text{ kHz} , \quad d'_M = 2.725(14) \text{ kHz},$$

and

$$eqQ/h = 223.38(18) \text{ kHz}.$$

The error limits shown for the hyperfine constants are large enough to be conservative estimates of the total probable error in the experiment. The calculated zero-field energy levels and transition frequencies based on these hyperfine parameters

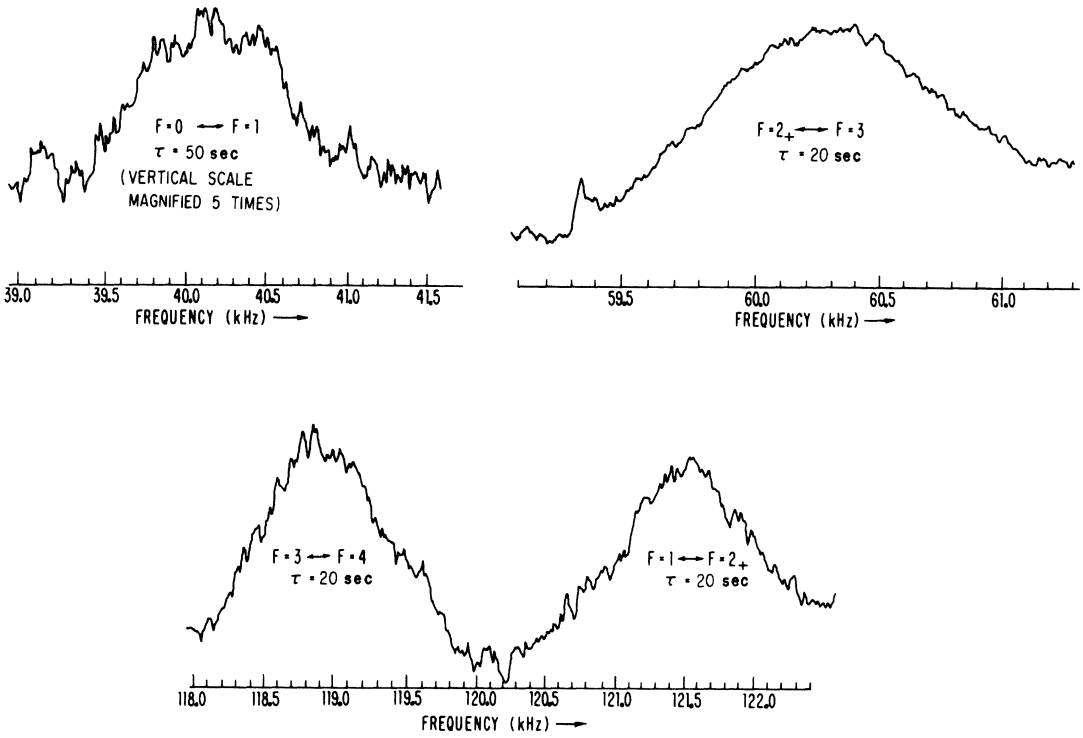

FIG. 10. Some of the zero-field transitions in the $J=2$ state of D_2.

are shown in Table IV.

Further improvements could be made in the determination of the hyperfine parameters in the $J=2$ state of D_2 by observing all six allowed transitions with a source temperature of 142 °K in a magnetically shielded low-field resonance region at least 2 m long. The overlap of the interference patterns would be eliminated, and better homogeneity of the external field could be obtained by using air-core rectangular coils for preserving the direction of quantization.

VII. EFFECTS OF NUCLEAR MOTION

To a first approximation, the differences of the hyperfine constants between the isotopic forms of the hydrogen molecule are explained by the differences in the multipole moments and masses of the nuclei. Ramsey has shown[8,9] that the remaining differences (as well as those that occur between different rotation-vibration states of the same isotopic form) are caused by the effects of nuclear

TABLE III. Experimental data on the $J=2$ state of D_2 in zero field.

Transition	rf current (A)	Observed frequency (kHz)	Corrected frequency (kHz)
$F=0 \leftrightarrow F=1$	10	40.256(35)	40.256(35)
$F=2_+ \leftrightarrow F=3$	9	60.146(20)	60.196(20)
$F=3 \leftrightarrow F=4$	8	118.999(25)	118.949(25)
$F=1 \leftrightarrow F=2_+$	7.5	121.606(20)	121.655(20)
$F=2_+ \leftrightarrow F=3$	7.5	60.146(20)	60.186(20)
$F=3 \leftrightarrow F=4$	7.5	118.968(25)	118.928(25)
$F=1 \leftrightarrow F=2_+$	7.5	121.620(20)	121.700(20)

TABLE IV. Calculated zero-field energy levels and allowed hyperfine transition frequencies in the second rotational state of D_2 assuming $c_d = 8.723$ kHz, $d_M' = 2.725$ kHz, and $eqQ/h = 223.380$ kHz.

Energy levels	
State	Energy (kHz)
$F=0$	−45.727
$F=1$	−5.418
$F=2_-$	−69.042
$F=2_+$	+116.225
$F=3$	+56.037
$F=4$	−62.911
Allowed transition frequencies	
Transition	Frequency (kHz)
$F=0 \leftrightarrow F=1$	40.310
$F=2_+ \leftrightarrow F=3$	60.187
$F=1 \leftrightarrow F=2_-$	63.625
$F=3 \leftrightarrow F=4$	118.948
$F=1 \leftrightarrow F=2_+$	121.643
$F=2_- \leftrightarrow F=3$	125.080

TABLE V. Spectroscopic constants of H_2, HD, and D_2 used for the averages over the nuclear motion.

Spectroscopic const.	H_2	HD	D_2
B_e (cm^{-1})	60.841	45.638	30.442
ω_e (cm^{-1})	4400.39	3811.92	(3112.93) [a]
a_1	−1.598	−1.595	(−1.592) [b]
a_2	+1.868	+1.854	(+1.840) [b]
a_3	−2.072	−2.047	(−2.022) [b]
a_4	+2.261	+2.250	(+2.239) [b]
R_e (Å)	0.74173	0.74173	(0.74173) [c]

[a]Calculated from ω_e of HD using the reduced mass based on the nuclear masses only.

[b]Estimated from the values of H_2 and HD assuming $a_i(H_2) - a_i(HD) = a_i(HD) - a_i(D_2)$.

[c]Stoicheff (Ref. 28) gives 0.74165 Å for R_e in D_2, but this is not as accurate as the values determined for HD and H_2.

motion. Using approximations similar to those of Born and Oppenheimer, he has expressed the hyperfine constants in terms of several basic functions of the internuclear separation R and has shown how these quantities may be averaged by Morse potential wave functions.

Recently, Schlier[10] and Herman[11] have derived the averaged values of up to the sixth power of the variable $\xi = (R - R_e)/R_e$ for various rotation-vibration states of a molecule in terms of the constants B_e and ω_e, and the Dunham parameters of the anharmonic potential $a_1, a_2, \ldots, a_5$. In the present calculations of the effects of nuclear motion on the hyperfine constants, Ramsey's basic functions of the internuclear distance have been expressed as power series in the variable ξ, and the average values were calculated from the equations in Ref. 11 because the Dunham parameters provide a more complete description of the internuclear potential in molecular hydrogen than the Morse potential is able to give.

The spectroscopic constants of the molecular isotopes of hydrogen were derived from the Raman spectra observed by Stoicheff[28] and are listed in Table V.

To determine the value of eqQ/h in the first rotational state of D_2, it is necessary to calculate the value of the direct magnetic spin-spin interaction constant d'_M from the spectroscopic constants of the molecule. This can be done directly from Eq. (18) by using the following series approximation for the value of the inverse cube of R:

$$\langle (R/R_e)^{-3} \rangle_J \approx \langle 1 - 3\xi + 6\xi^2 - 10\xi^3 + 15\xi^4 - 21\xi^5 + 28\xi^6 \rangle_J . \quad (23)$$

As a test of the accuracy of the calculation of d'_M in the first rotational state of D_2, the values of d'_M were calculated for the first rotational state of H_2 and HD and for the second rotational state of D_2 and then compared with the observed values. The results of this comparison are shown in Table VI. Since the calculations are in good agreement with the observed values of d'_M, the value of d'_M for the first rotational state of D_2 will be taken to be

$$d'_M = 2.737(1)\ \text{kHz} .$$

TABLE VI. Comparison of the calculated and observed values of d'_M.

Quantity	H_2 ($J = 1$)	HD ($J = 1$)	D_2 ($J = 1$)	D_2 ($J = 2$)
$\langle (R/R_e)^{-3} \rangle_J$	0.97965	0.98290	0.98654	0.98195
d'_M(calc.)(kHz)	115.346	17.765	2.737_0	2.724_4
d'_M(obs.)(kHz)	115.342(48) (Ref. 2)	17.761(12) (Ref. 5)	···	2.725(14) (Present work)

The electric quadrupole coupling constant can now be determined from Eq. (16) using the best estimate of the constant d for the $J = 1$ state of D_2 given in Sec. V. The result is that

$$eqQ/h = 225.044(24)\ \text{kHz}$$

for the $J = 1$ state of D_2. This result is the most accurate value of a deuteron electric quadrupole coupling constant in molecular hydrogen that is presently available.

It is interesting to compare the three experimental determinations of the electric quadrupole interaction constant in the $J = 1$ state of Hd and in the $J = 1$ and $J = 2$ states of D_2 as a test of the present theoretical calculations of the electric field gradient at the nuclei in the hydrogen molecule. The most recent theoretical value of the electric field gradient has been calculated by Narumi[7] using an eleven-term James-Coolidge wave function. The values of $q'(r) = (1/2e)\partial^2 V^e/\partial z_0^2$ are tabulated in atomic units

TABLE VII. Comparison of the electric quadrupole interactions in HD and D_2.

Quantity	HD ($J = 1$)	D_2 ($J = 1$)	D_2 ($J = 2$)
Experimental eqQ/h (kHz)	224.540(60) (Ref. 5)	225.044(24) [a]	223.380(180) [a]
$\langle q'(R) \rangle_J$ (a.u.)	0.17102(21) [b]	0.17113(19) [b]	0.16991(18) [b]
Q_d (mb)	2.7939(40) [c]	2.7983(30) [c]	2.7975(60) [c]
"Equivalent" value of eqQ/h from the $J = 1$ state of D_2	224.892(80) [d]	···	223.442(50) [d]

[a]Present work.

[b]Error due to interpolation function only.

[c]Error estimate includes observational error and errors due to interpolation function.

[d]Error estimate includes observational error and the uncertainty in the calculated ratios of the average electric field gradients.

for $R = 1.2$, 1.3, 1.4, and 1.5 Bohr radii. Narumi stated that the largest source of error in his calculation was introduced by the interpolation formulas used for $q'(R)$ and by his method of averaging these interpolation formulas over the nuclear motions. Therefore, the values of ${}^{x}_{v}\langle q'(R)\rangle_J$ were recalculated in the present work using several different interpolation formulas, the improved spectroscopic constants of Table V, and the averaging technique of Schlier and Herman. Since the effects of nuclear motion are small, the average values ${}^{x}_{v}\langle q'(R)\rangle_J$ tend to be correlated for a particular interpolation function. The ratios of the average field gradients are less dependent on the method of interpolation than are the absolute values of ${}^{x}_{v}\langle q'(R)\rangle_J$. Therefore, in addition to calculating the values of Q_d from the three observed values of eqQ/h, "equivalent" values of eqQ/h for the $J=1$ state of HD and the $J=2$ state of D_2 were calculated from the observed values in the $J=1$ state of D_2.

The electric quadrupole interactions in HD and D_2 are compared in Table VII. There is good agreement between the observations in the $J=1$ and $J=2$ states of D_2, but there is evidence of some discrepancy with the observation in the $J=1$ state of HD. Not only is the determination of Q_d slightly lower in HD, but the observed value of eqQ/h is some 350 Hz lower than the "equivalent" value predicted from the $J=1$ state of D_2. This difference may originate either from truncation errors in the adiabatic method of averaging over the effects of nuclear motion which have not been considered here, or from nonadiabatic effects of the nuclear motion. Although different anharmonic potentials were used for HD and D_2, the differences were so small that they would not significantly affect the predicted value of eqQ/h for Hd. The center of mass in HD does not coincide with the center of electric charge, and it is possible that nonadiabatic effects could reduce the average value of the electric field gradient at the deuteron in HD. Further work on the theoretical electric field gradient in hydrogen molecules would be of interest in determining a more accurate value of Q_d, which is a very fundamental quantity in nuclear physics, as well as investigating whether the nonadiabetic effects of nuclear motion are significant at the present level of experimental accuracy.

The variation of the spin-rotation interaction constants in the isotopic forms of molecular hydrogen also presents some unresolved theoretical problems. In their experiment on HD,[5] Quinn *et al.* reported that the Wick portion of the spin-rotation constants for the proton and deuteron in HD were not exactly proportional to the g factors of the nuclei as had been expected. The origin of this difference is still not fully understood.

The usual decomposition of the spin-rotation interaction constants in the molecular hydrogen isotopes is written as

$$ {}^{x}(c_n)_{\rm obs} = {}^{x}_{v}\langle c_{NA}\rangle_J + {}^{x}_{v}\langle c_N{}^{\rm nuc}\rangle_J + {}^{x}_{v}\langle c_N{}^{\rm el}\rangle_J , \qquad (24) $$

where the first term is Ramsey's nuclear acceleration correction,[9] the second term is the contribution of the relative circulation of the charge of the other nucleus about the nucleus N, and the third (high-frequency) term is the contribution from the circulation of the electrons.

For the purposes of the present calculations, it was assumed that the third (electronic) term of Eq. (24) was different for protons than for deuterons in the molecular hydrogen isotopes. This is reasonable because the protons are lighter and have larger zero-point vibrational amplitudes than the deuterons. However, the nuclear part of the spin-rotation interaction constant was calculated the same way for protons as for deuterons. This calculation requires only the average value of $(R/R_e)^{-3}$, which has been shown in Table VI to be calculated consistently for the hydrogen isotopes. Also, the standard corrections for the effects of the acceleration of the nucleus were made for both the proton and the deuteron.

The first two terms of Eq. (24) were calculated

TABLE VIII. Calculated values of terms in the spin-rotation interaction constants and the high-frequency part of the nuclear shielding constants in molecular hydrogen.

Quantity	H_2 ($J=1$)	p in HD ($J=1$)	d in HD ($J=1$)	D_2 ($J=1$)	D_2 ($J=2$)
C_N (kHz)	113.904(30) (Ref. 2)	85.600(18) (Ref. 5)	13.122(11) (Ref. 5)	8.768(3)[a]	8.723(20)[a]
${}^{x}_{v}\langle C_{NA}\rangle_J$ (kHz)	1.072	0.946	0.037	0.031	0.025
${}^{x}_{v}\langle C_N{}^{\rm nuc}\rangle_J$ (kHz)	206.509	155.421	23.858	15.970	15.895
${}^{x}_{v}\langle C_N{}^{\rm el}\rangle_J$ (kHz)	−93.678	−70.767	−10.773	−7.232	−7.197
10^6 ${}^{x}_{v}\langle \sigma_N{}^{\rm hf}\rangle_J$	−5.63(8)[b]	−5.65(8)[b]	−5.61(8)[b]	−5.64(8)[b]	−5.63(8)[b]

[a]Present work.

[b]Error estimated from calculation of ${}^{H_2}_{0}\langle C_N{}^{\rm el}\rangle_1$ given in text.

by the present method of averaging the nuclear motion in terms of the Dunham parameters of the molecules in a similar fashion as described in Refs. 8 and 9 for a Morse potential. The remaining electronic term was then evaluated from the observed value of the particular spin-rotation constant by subtraction. The dependence of the electronic (high-frequency) part of the spin-rotation constant on R was determined by fitting a quadratic polynomial in ξ to the three observed values for the deuteron nuclei in the molecular hydrogen isotopes.

It was then assumed that the electronic part of the spin-rotation interaction had the same dependence on R for the protons and the deuterons, but that its value differed for the protons relative to the deuterons by the same amount as the ratio of the electronic part of the average rotational magnetic field at the two nuclear sites in HD. The electronic part of the spin-rotation interaction constant in H_2 could then be calculated from the value derived experimentally for the proton in HD, and then compared with the experimentally determined value for H_2. The value of ${}^{H2}_{0}\langle c_p{}^{el}\rangle_1$ was calculated to be -93.810 kHz, which agrees reasonably well with the experimentally determined value of -93.678 kHz. If no corrections were made for averaging over the nuclear motion in the calculation of ${}^{H2}_{0}\langle c_p{}^{el}\rangle_1$ from the observed value in HD, there would be approximately a 0.65-kHz difference with the experimentally determined value. Therefore, the assumptions that have been made on the internuclear dependence of the spin-rotation constant agree well with the observations.

The electronic part of the spin-rotation constant is related[8] to the high-frequency part of the nuclear shielding constant ${}^{x}_{v}\langle\sigma_N{}^{hf}\rangle_J$. The values of ${}^{x}_{v}\langle\sigma_N{}^{hf}\rangle_J$ were calculated from the values of ${}^{x}_{v}\langle c_N{}^{el}\rangle_J$ using the present averaging method in analogy with the calculations in Ref. 5. The results are listed in Table VIII along with the summary of the calculations for the spin-rotation interaction constants. The results for the high-frequency contributions to the nuclear shielding constants should be compared to those given by Quinn *et al.*[5] as ${}^{HD}_{0}\langle\sigma_d{}^{hf}\rangle_1 = -5.91(30)\times10^{-6}$ and ${}^{HD}_{0}\langle\sigma_p{}^{HD}\rangle_1 = -5.96(30)\times10^{-6}$. The difference between these determinations and the present values arises from the method used to establish the electronic part of the spin-rotation interaction constant and its dependence on the internuclear distance.

The calculations in this section have shown that the present experimental accuracy in measuring some of the hyperfine constants in the isotopes of molecular hydrogen is greater than that of the existing methods of accounting for the effects of nuclear motion. Further experiments should be considered for molecular tritium and for the nonradioactive isotopes at greater precision. With better data on all isotopic forms of molecular hydrogen, it will be possible to improve the understanding of the effects of nuclear motion on the hyperfine interactions in the hydrogen molecule.

---

†Work supported in part by the National Science Foundation and the Office of Naval Research.

*Holder of a National Research Council (Canada) postgraduate scholarship. Present address: Department of Physics, University of Toronto, Toronto 181, Ontario, Canada.

[1]J. M. B. Kellogg, I. I. Rabi, N. F. Ramsey, and J. R. Zacharias, Phys. Rev. 56, 728 (1939).

[2]N. J. Harrick, R. G. Barnes, P. J. Bray, and N. F. Ramsey, Phys. Rev. 90, 260 (1953).

[3]R. G. Barnes, P. J. Bray, and N. F. Ramsey, Phys. Rev. 94, 893 (1954).

[4]I. Ozier, P. N. Yi, A. Khosla, and N. F. Ramsey, Bull. Am. Phys. Soc. 12, 132 (1967).

[5]W. E. Quinn, J. M. Baker, J. T. LaTourrette, and N. F. Ramsey, Phys. Rev. 112, 1929 (1958).

[6]R. F. Code and N. F. Ramsey, Rev. Sci. Instr. 42, 896 (1971).

[7]H. Narumi and T. Watanabe, Progr. Theoret. Phys. (Kyoto) 35, 1154 (1966).

[8]N. F. Ramsey, Phys. Rev. 87, 1075 (1952).

[9]N. F. Ramsey, Phys. Rev. 90, 232 (1953).

[10]C. Schlier, Fortschr. Physik 9, 455 (1961).

[11]R. M. Herman and S. Short, J. Chem. Phys. 48, 1266 (1968); 50, 572E (1969).

[12]N. F. Ramsey, in *Recent Research in Molecular Beams*, edited by I. Esterman (Academic, New York, 1959), pp. 107.

[13]N. F. Ramsey, *Molecular Beams* (Clarendon Press, Oxford, 1956).

[14]H. Harrison, D. G. Humma, and W. L. Fite, J. Chem. Phys. 41, 2567 (1964).

[15]J. H. Shirley, J. Appl. Phys. 34, 783 (1963).

[16]F. Bloch and A. Siegert, Phys. Rev. 57, 522 (1940).

[17]M. R. Baker, H. M. Nelson, J. A. Leavitt, and N. F. Ramsey, Phys. Rev. 121, 807 (1961).

[18]I. Ozier, Ph.D. thesis (Harvard University, 1965) (unpublished).

[19]P. N. Yi, Ph.D. thesis (Harvard University, 1967) (unpublished).

[20]J. I. Musher, Phys. Rev. Letters 15, 1015 (1965); 16, 675E (1966).

[21]I. Ozier, L. M. Crapo, and N. F. Ramsey, J. Chem. Phys. 49, 2314 (1968).

[22]H. Benoit and P. Piejus, Compt. Rend. 265B, 101 (1967).

[23]C. M. Dutta, N. C. Dutta, and T. P. Das, Phys. Rev. Letters 25, 1695 (1970).

[24]N. F. Ramsey, Phys. Rev. 85, 60 (1952).

[25]G. H. Fuller and V. W. Cohen, *Nuclear Moments* (Nuclear Data Project, Oak Ridge, Tenn., 1965).

[26]A. R. Edmonds, *Angular Momentum in Quantum Mechanics* (Princeton U. P., Princeton, N. J., 1960).

[27]M. Rotenberg, R. Bivins, N. Metropolis, and J. K. Wooton, Jr., *The* $3-j$ *and* $6-j$ *Symbols* (MIT, Cambridge, Mass., 1959).

[28]B. P. Stoicheff, Can. J. Phys. 35, 730 (1957).